A single three-parameter tilted fibre Bragg grating sensor to monitor the thermosetting composite curing process

Fazzi, Luigi; Struzziero, Giacomo; Dransfeld, Clemens; Groves, Roger Michael

DOI
10.1080/20550340.2022.2041221

Publication date
2022

Document Version
Final published version

Published in
Advanced Manufacturing: Polymer and Composites Science

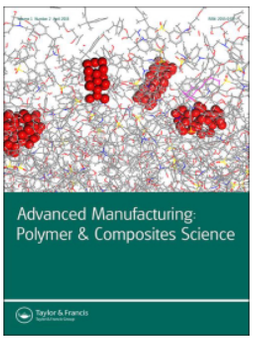

Taylor & Francis
Taylor & Francis Group

Advanced Manufacturing: Polymer & Composites Science

ISSN: (Print) (Online) Journal homepage: https://www.tandfonline.com/loi/yadm20

A single three-parameter tilted fibre Bragg grating sensor to monitor the thermosetting composite curing process

Luigi Fazzi, Giacomo Struzziero, Clemens Dransfeld & Roger Michael Groves

To cite this article: Luigi Fazzi, Giacomo Struzziero, Clemens Dransfeld & Roger Michael Groves (2022) A single three-parameter tilted fibre Bragg grating sensor to monitor the thermosetting composite curing process, Advanced Manufacturing: Polymer & Composites Science, 8:1, 33-41, DOI: 10.1080/20550340.2022.2041221

To link to this article: https://doi.org/10.1080/20550340.2022.2041221

Published online: 15 Feb 2022.

ADVANCED MANUFACTURING: POLYMER & COMPOSITES SCIENCE
2022, VOL. 8, NO. 1, 33–41
https://doi.org/10.1080/20550340.2022.2041221

A single three-parameter tilted fibre Bragg grating sensor to monitor the thermosetting composite curing process

Luigi Fazzi[a], Giacomo Struzziero[b,c], Clemens Dransfeld[c] and Roger Michael Groves[a]

[a]Faculty of Aerospace Engineering, Structural Integrity and Composites Group, Delft University of Technology, Delft, The Netherlands; [b]Mechanical Systems Engineering Laboratory, Swiss Federal Laboratories for Materials Science and Technology, Duebendorf, Switzerland; [c]Faculty of Aerospace Engineering, Aerospace Manufacturing Technologies Group, Delft University of Technology, Delft, The Netherlands

ABSTRACT

The unique sensing features of the tilted Fibre Bragg Grating (TFBG) as a single three-parameter optical sensor are demonstrated in this work, to monitor the manufacturing process of composite materials produced using Vacuum Assisted Resin Transfer Moulding (VARTM) process. Each TFBG sensor can measure simultaneously and separately strain, temperature and refractive index (RI) of the material where the optical fibre is embedded. A TFBG embedded in a 2 mm glass-fibre/epoxy composite plate was used to measure the thermomechanical variations induced during the curing process. At the same time, the RI measurements, performed with the same TFBG sensor, can estimate the degree of cure of the resin. The TFBG sensor shows to be a valid and promising technology to improve the state of art of sensing and monitoring in composite material manufacturing.

KEYWORDS

Sensors; curing of polymers; strain; composites; thermosets

GRAPHICAL ABSTRACT

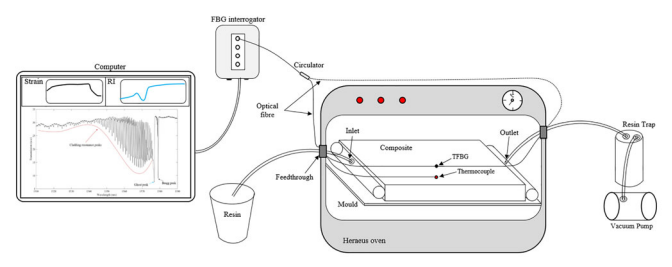

1. Introduction

Composite materials are widely used in different engineering sectors such as aerospace, aeronautics, automotive, naval, wind turbines and railways [1] since their high strength to weight ratio and anisotropic nature brings several advantages compared to traditional engineering materials. In particular, the use of composite in primary structures has allowed significant weight reduction while maintaining the same mechanical performance in the aeronautic sector. In the last decades, a significant weight reduction has been achieved by replacing solid metallic parts with composite material [2]. Nevertheless, several defects can be introduced due to a poorly designed manufacturing practice. This can lead to unacceptable level of defects and rejection of the part, which poses cost and sustainability issues [3,4]. Therefore, inspection techniques to investigate the internal state of composites during manufacturing have been developed. Since the first monitoring technologies appeared, Optical Fibre (OF) sensing immediately proved to be a valid option [5], and specifically, Fibre Bragg Grating (FBG) sensors are the most used OF sensors for embedded real-time monitoring of composite structures. They provide accurate and reliable remote multi-parameter measurements (temperature, strain, pressure, etc.), low weight, minimal intrusiveness and high installation flexibility, and additionally, they are immune to electromagnetic interference [6]. Since the 2000s, the embedding of OF sensors has been performed for composites manufacturing quality control [7–10], as it is a fundamental step to obtain the best mechanical performance [11]. Due to dominant heat transfer phenomena and low thermal conductivity

CONTACT Luigi Fazzi l.fazzi@tudelft.nl Structural Integrity and Composites Group, Faculty of Aerospace Engineering, Delft University of Technology, Delft 2629 HS, The Netherlands

through thickness, some defects such as voids, temperature overshoots, residual stresses and part deformation can occur during composite manufacturing process, which can significantly lower the mechanical performances of the components. A significant effort on the optimisation of the composite manufacturing processes has been undertaken to minimise the occurrence of such defects [12–16]. Moreover, the monitoring of a specific manufacturing process stage is necessary to avoid unexpected defects to arise. At the same time, multiple sensors strategy is not desirable as their presence can generate defects or influence the material mechanical performance, and it would increase the cost and, hardware and software complexity. Some solutions have been developed by considering the benefits of the OFs using a combination of similar and/or hybrid sensors in the same waveguide able to compensate or perform dual-parameter measurements [17–24]. However, they suffer from several drawbacks which make them unattractive, such as non-localized measurements, poor spatial resolution and accuracy, use of an intrusive capsule and time consuming. TFBGs are characterised to have a Bragg grating structure tilted with respect to the optical axis of the OF. This special imposition allows a spectrum composed of several well-defined resonance peaks to be obtained [25]. By exploiting these peaks in the TFBG, after a calibration step, each single TFBG sensor can be used to measure, simultaneously and separately, the variation of strain, temperature and Refractive Index (RI) at the point where it is embedded [26]. Specifically, the RI variation of the resin during its curing stage can be monitored and associated with its degree of cure [27]. However, there are no works proving that the TFBG can perform simultaneous three parameter measurements when embedded in a composite and that a single sensor is sufficient to monitor the thermomechanical and curing state of the material.

In the present paper a single three-parameter optical sensor based on a weakly Tilted FBG (TFBG) is demonstrated to monitor the thermomechanical state and the degree of cure of a thermosetting composite during the Vacuum Assisted Resin Transfer Moulding (VARTM) manufacturing process. The simultaneous temperature, strain and RI measurements with a single embedded TFBG during the curing stage of a 2 mm composite, are reported with a section dedicated to the comparison between the degree of cure and the RI trend during the curing time.

2. TFBG sensing theory

In a short period tilted grating the periodic and permanent RI modulation of the OF core, is deliberately tilted with respect to the longitudinal axis of the waveguide [28]. The tilt angle (θ) is super-imposed during the Bragg grating writing process through tilting parts of the FBG manufacturing machine [25]. This angle enhances the generation of multiple peaks in the TFBG spectrum [29]. Specifically, in this paper, only reflective weakly TFBGs ($\theta < 15°$) are considered since, apart from the Bragg and the cladding resonance peaks, they have a further peak in their spectrum called the Ghost resonance, which allows the measurement of multiple parameters simultaneously [25–31]. All the resonance peaks in the spectrum are sensitive in different measure to thermomechanical external perturbations, which cause a shifting variation of the nominal peak wavelength. However, the Bragg and Ghost peaks are immune to external RI variations, while the cladding resonances undergo a wavelength shift and amplitude change when this is varying. Considering these aspects and by performing a preliminary calibration, both the Bragg and the Ghost peaks can be used to measure simultaneously and separately the temperature and the strain variation from a reference condition. At the same time, the area generated by the envelope of the lower and upper cladding resonance peaks can be exploited to measure independently the variations of the RI surrounding the TFBG sensor [8,31,32].

Once the sensitivity coefficients (K_ε, K_T) of the Bragg and Ghost peaks are obtained from the calibration, their wavelength shifting ($\Delta\lambda_{\text{Bragg}}$, $\Delta\lambda_{\text{Ghost}}$) are used to measure separately the strain ($\Delta\varepsilon$) along the OF axis and temperature (ΔT) variations using the K global thermomechanical sensing matrix [33]. This technique is based on the peaks wavelength shifts acquired through the FBG interrogator device, which can detect data points with a certain scanning wavelength resolution (*swR*). Consequently, *swR* also influences the sensor thermal resolution, which can be calculated through the ratio between the thermal sensitivity coefficients difference and *swR*. The measurements were performed by respecting this resolution constraint, which omission implies incorrect calculations.

Regarding the surrounding RI, the cladding resonance peaks envelope area is calculated using the Delaunay triangulation (D-T) demodulation technique [31]. During the refractometric calibration, the area values are calculated and correlated at each external RI change and normalised with respect to a reference area value. At this point, from the correlation points, a fitting function can be obtained in relation to the external RI range of interest. Hence, the surrounding RIs can be obtained by solving the fitting function with respect to the normalised envelope area of the TFBG immersed in a medium. This

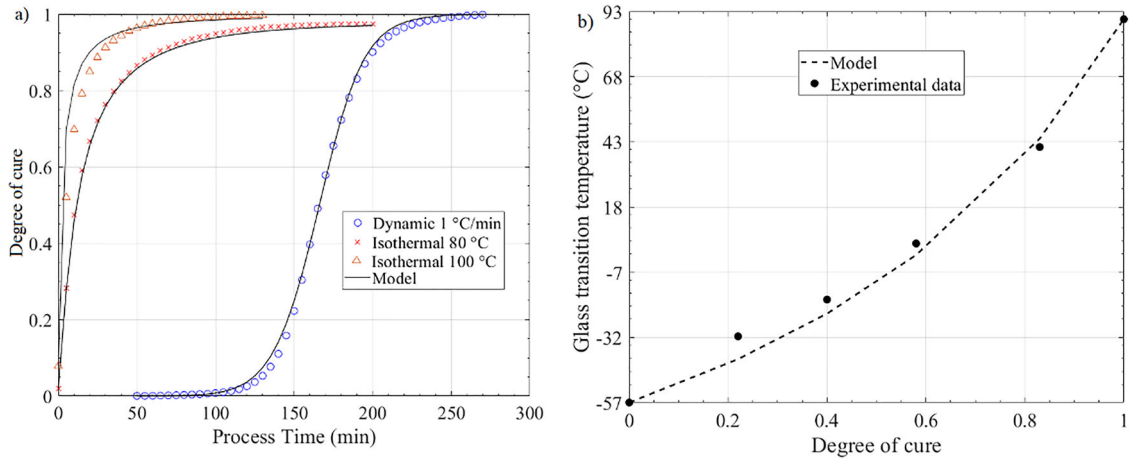

Figure 1. Epikote™ 04908/Epikure™ 04908 system phenomenological models fitting a) Cure kinetics and b) Di Benedetto equation.

process and the D-T technique are treated in more detail in [31].

3. Experimental

In the following section 3.1 provides details on the reinforcement fibre and matrix, and the TFBG sensor used to perform the measurements inside the composites, while section 3.2 treats the cure kinetics and T_g characterisation. Section 3.3 provides details on the VARTM process and sensor embedding stage.

3.1. Materials and sensors

The 2 mm thick composite plate (12 plies) was manufactured using Interglass™ Unidirectional (UD) S-glass fibre (220 gr/m^2, 92145) plies and epoxy resin. The resin system was a low temperature curing Hexion Epikote™ 04908 epoxy resin mixed with Epikure™ Hardener 04908 (mixing ratio resin/hardener 100:30 parts by weight) [34]. The vacuum bag setup consisted of a nylon film Wrightlon® 7400, sealant tape Solvay LTS90B, infusion mesh Airtech Greenflow 75, peel ply Airtech Stitch Ply A and release perforated polyolefin foil Wrightlon® WL3700. The TFBG sensor embedded in the composite, was manufactured by FORC-Photonics in Fibercore PS1250/1500 OF with a 2° tilt angle, and is 4 mm long with a 10 mm uncoated length. The TFBG signal was acquired by using the FBG interrogator NI PXIe-4844, which has a $swR = 4$ pm and a maximum sample frequency of 10 ± 0.1 Hz. A thin K-thermocouple (TC, Ø = 0.250 mm) was also embedded close to the TFBG to provide a temperature measurement reference for comparison with the TFBG measurements. The TC has an accuracy of ±1 °C. The integration details are reported in section 3.3. Before TFBG embedding, the thermomechanical calibration of the TFBG sensor was performed as in [33]. The strain and temperature sensitivity coefficients found are $K\varepsilon_{,Bragg}$=1.255 ± 0.004 pm/$\mu\varepsilon$ and $K\varepsilon_{,Ghost}$=1.255 ± 0.006 pm/$\mu\varepsilon$ while $KT_{,Bragg}$=8.686 ± 0.012 pm/°C and $KT_{,Ghost}$=9.2 ± 0.014 pm/°C.

The RI calibration procedure of the TFBG was performed as described in [35], with the room temperature kept at 20 ± 1.5 °C. Usually the epoxy resins suitable for VARTM processes have a RI range 1.5-1.56 [36] when uncured, which is expected to increase during the curing stage [27]. For the resin used in this study, the RI of the uncured resin is around 1.54 at 25 °C [34]. Hence, to obtain the best measurement accuracy, the curve branch in the range 1.46-1.7 was fitted by a fifth-order polynomial function with a fitting square error (R^2) of 0.9996, where the worst RI accuracy is 1×10^{-3} at 1.5.

3.2. Cure kinetics and T_g characterisation

The cure kinetics characterisation of the epoxy system was carried out with a TA Instrument Differential Scanning Calorimeter (DSC) 2500. The DSC used liquid nitrogen with a flow rate of 10 ml/min. Two isothermal tests at 80 °C and 100 °C and one dynamic test at 1 °C/min were performed. The glass transition temperature evolution was characterised using Modulated Differential Scanning Calorimetry (MDSC), at a 3 °C/min ramp rate with a modulation set at 1 cycle/min and an amplitude of 1 °C, by observing the evolution of the reversible components of the specific heat. Next to the fully cured and fully uncured samples, four partially cured samples were manufactured by heating uncured resin samples at 1 °C/min up to an increasing final temperature followed by a quick cool down at the fastest possible machine rate of about 50 °C/min to stop the reaction from progressing. To validate the cure kinetics model, two additional samples have been partially cured. The cure profiles used dictated a ramp-up to 80 °C at 1 °C/min followed by

Table 1. Fitting parameters values for the cure kinetics and glass transition temperature material models of Epikote™ 04908/Epikure™ 04908 system.

Parameters	A	E	n	m	C	α_c	α_T	H_{tot}	T_{go}	$T_{g\infty}$	λ
Values	21594	49400	1.58	0.05	80	0.44	0.0015	760	−57	90	0.453
Units	s^{-1}	$Jmol^{-1}$					K^{-1}	Jg^{-1}	°C	°C	

an isothermal dwell of 20 min for the first sample and 40 min for the second. After that, the samples have been quickly cooled down to stop the reaction. An MDSC analysis to identify the glass transition temperature of the sample has been subsequently performed. The resin cure kinetics and Di Benedetto equation were fitted to the experimental results as shown in the following section.

3.2.1. Degree of cure and Di benedetto equation

The degree of cure and the glass transition temperatures trend are obtained from the experimental data. These have been fitted with the following kinetics model proposed by Khoun *et al.* [37], the model proved to accurately describe similar epoxy resin systems [14]:

$$\frac{d\alpha}{dt} = \frac{Ae^{\left(\frac{-E}{RT}\right)}}{1+e^{C(\alpha-\alpha_c-\alpha_T T)}}(1-\alpha)^n\alpha^m, \quad (2)$$

where α is the degree of cure, α_c, α_T, are coefficients controlling the transition of the kinetics from chemical to diffusion; C governs the breadth of the transition into the diffusion controlled regime, m and n are reaction orders for the n-*th* order and autocatalytic terms, A is a pre-exponential Arrhenius factor, E is the activation energy of the Arrhenius functions, T is the absolute temperature, and R is the universal gas constant. Figure 1a shows the fitting of the experimental data with the proposed phenomenological kinetic model. The average relative error of the fitting is about 2%. The heat generated Q by the exothermic reaction can be calculated as follows:

$$Q = \rho_r v_r H_{tot}\frac{d\alpha}{dt}, \quad (3)$$

Where ρ_r is the resin density, v_r the volume resin fraction and H_{tot} is the total enthalpy. The glass transition temperature model to fit the experimental data follows the Di Benedetto equation [38]:

$$T_g = T_{go} + \frac{(T_{g\infty}-T_{go})\lambda\alpha}{1-(1-\lambda)\alpha}, \quad (4)$$

here $T_{g\infty}$ and T_{go} are the glass transition temperatures of the fully cured and uncured material respectively and λ is a fitting parameter governing the convexity of the dependence. Figure 1b illustrates the fitting of the experimental data with the Di Benedetto equation.

Table 1 reports the fitting parameters of the cure kinetics and glass transition temperature development models. The two validation samples resulted in glass transition temperatures of 25 °C and 45 °C, according to the Di Benedetto model developed, this corresponds to degrees of cure of 0.74 and 0.84, respectively. The degree of cure prediction using the cure kinetics model developed is for 0.77 and 0.86 degree of cure, proving that the model predicts the degree of cure development of the resin system studied within 4% accuracy.

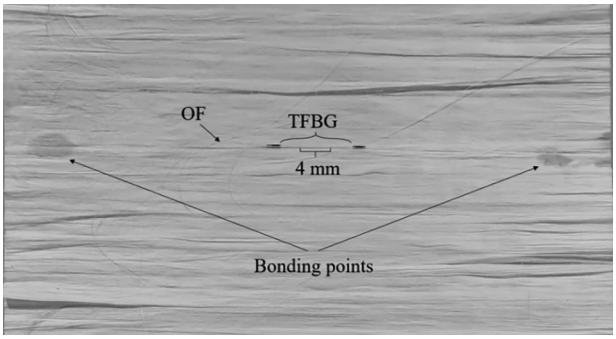

Figure 2. Positioning and gluing of a TFBG sensor on a reinforcement ply.

3.3. VARTM process

The VARTM manufacturing process was used to produce the samples and consists of an infusion stage followed by a curing stage. The OF was placed parallel to the UD reinforcement fibres layers of the composite to measure longitudinal strain. The mould was a flat aluminium plate (50x50x1 cm). The resin was infused at room temperature. The TFBG was embedded using the same translation stage of the TFBG calibration, to hold the TFBG straight and in the centre position of the reinforcement layer inducing a small pre-tensile force to the OF. The TFBG was then spot-glued on the glass-fibre foil using small drops of cyanoacrylate glue close to the edges of the composite layer (Figure 2). Additionally, a TC was placed as close as possible to the glued TFBG sensor by using a special web adhesive which melts once the resin covers it and, in a way that does not interfere with the material surrounding the OF sensor. The TFBG and TC were embedded in the middle plane (6^{th} reinforcement layer), after this, the preform can be assembled. Figure 3 gives a schematic view of the sample with the sensors embedded. The OFs and the TC wires exiting from the composite were protected with vacuum bag sealant tape.

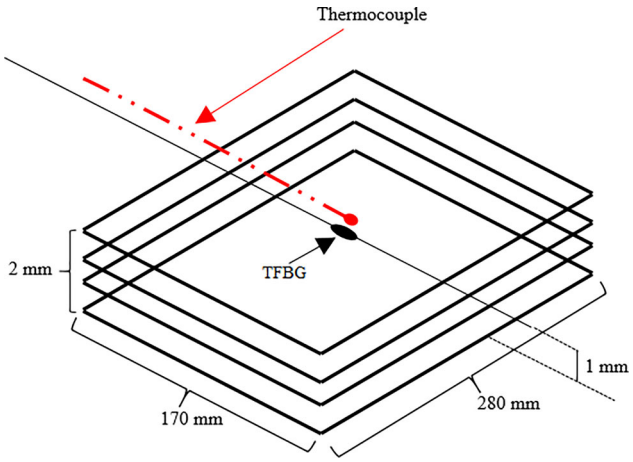

Figure 3. Schematic of the composite sample with TFBG sensor and TC.

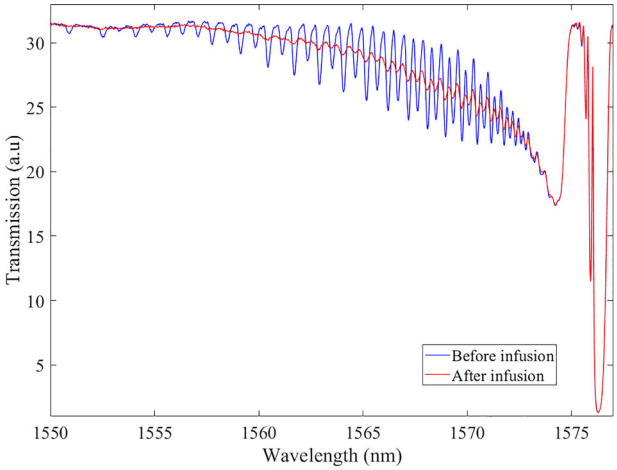

Figure 4. TFBG transmitted spectrum before (black) and after (red) incorporation in resin flow.

Resin infusion was performed at 50 mbar to avoid the evaporation of volatiles. During resin flow, the TFBG sensor was used to provide information on the flow arrival time whose details are reported in section 4.1.

After completing the infusion, the inlet line was closed and the panel was cured in an oven provided with an access hole from which the infusion lines, the OFs and the TCs can be externally connected. The applied curing temperature profile is suggested by the resin manufacturer [34]. As no indications are given by the manufacturer regarding ramp rates, a heating-up of 1 °C/min and cooling-down by natural convection were imposed to have a gradual temperature variation. The strain, temperature and RI measurements were performed by processing the TFBG spectra acquired during the curing time and these are reported in the results section.

4. Results and discussion

This section reports the outcomes of the TFBG measurements from the spectra acquired during the different stages of the VARTM process. In section 4.1, the TFBG spectra are analysed during the resin infusion stage. The results during the curing stage of the composite plate are addressed in section 4.2.

4.1. TFBG detection during resin infusion stage

During the infusion stage, the TFBG spectra can be used to monitor the resin flow front arrival. At this stage, the TFBG spectra were acquired every second, while the TC was recorded every 3 s. When the resin starts to wet the sensors, the depth between the upper and lower cladding peaks decreases uniformly until they reach a stable condition when the TFBG is fully immersed. In this last condition, the normalised envelope area returns the resin RI using the fitting correlation function obtained from the calibration. A detailed analysis of this behaviour can be found in [35]. Figure 4 shows the TFBG spectra before and after the resin flows in the thin composite. In this case, the required time for the resin to contact the sensor from the start of the infusion was ~50 s whilst to have a stable spectrum at the relative area, ~9 s were needed. The latter can be considered as the interval needed for the resin flow front to fully cover the TFBG after reaching it. However, this time should not be confused with the absolute speed in a single direction of the composite. In fact, due to the presence of the flow media on top, the flow front propagation is non uniform through the thickness as its permeation from the flow media is superposed to the in-plane flow. Moreover, small oscillations can be present in the spectrum due to pores migration flowing along the OF surface where the TFBG is present and influencing its coupling mode system locally. In this context, the TFBG spectral signals may be used to locally identify possible defects deriving from poor or incomplete wetting. This can occur on-line since the operations to calculate the envelope area are usually fast enough to be completed within the minimum refresh time of the device used to interrogate the TFBG sensors. Furthermore, as the time interval to obtain the spectrum of the single TFBG from dry to fully wet condition, can be calculated with an accuracy of 0.33 s (depending on the interrogator device), these sensors may be used to investigate the local permeability of a fibre reinforcement layer along the embedding direction.

4.2. TFBG measurements during curing stage

The composite thermomechanical state can be obtained with the TFBG as described in section 2. From this procedure, $\Delta\varepsilon$ and ΔT can be obtained from the moment in which the oven was switched-on (i.e. 96 min). At this point, the strain variation is

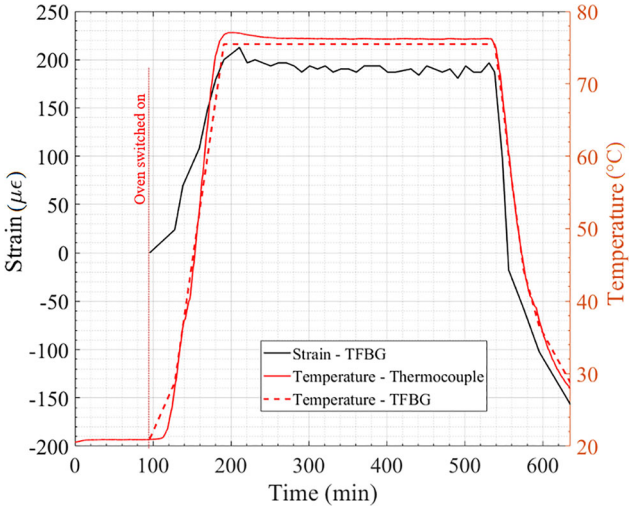

Figure 5. Temperature and strain trends during the composite curing time measured trough the embedded TFBG and TC.

assumed to be zero and the temperature is ∼21 °C. Here, the TFBG acquisition frequency is once per minute, while the TC measurements are every 3 s. Figure 5 shows the temperature (dashed red line) and strain (black continuous line) profiles measured by the embedded TFBG sensor.

Though the TFBG measurements performance are constrained to its thermal resolution (7.8 °C), here the temperature trends measured by the TC and TFBG are similar. Nevertheless, the TFBG thermal resolution generates an average temperature difference between the TC and TFBG temperature trends (red lines in Figure 5) of ∼0.78 °C, while the maximum difference is ∼1.7 °C at 198 min. As a consequence, since strains are calculated in isothermal conditions when the TFBG measures the maximum temperature, a mean and maximum strain deviation of ∼5 $\mu\varepsilon$ and ∼12 $\mu\varepsilon$ respectively, can be calculated through temperature differences. Considering the $\Delta\varepsilon$ and ΔT variations involved in Figure 5, the previous deviations can be considered negligible. The strain oscillations detected by the TFBG along the entire interval between 200 and 540 min, are caused by temperature fluctuations. During the cooling down step, the TFBG measurements were stopped when the temperature reached 28.8 °C as lower temperatures were not detectable due to the TFBG thermal calibration. At this temperature the strain measured by the TFBG is around -157 $\mu\varepsilon$. However, the lowest detected temperature was 23.7 °C. The additional 5.1 °C correspond to about -23 $\mu\varepsilon$ hence, the maximum $\Delta\varepsilon$ expected is around -180 $\mu\varepsilon$. The compressive strain measured is a combination of compressive strains due to matrix related shrinkage and contraction in the cool down phase due to coefficient of thermal expansion (CTE) [15].

The resin RI can be evaluated through the embedded TFBG at any moment of the manufacturing process, simultaneously with the strain and temperature measurements, after being immersed by the resin flow. In Figure 6, the envelope area and the resin RI evolution is shown with the TC temperature profile where both parameters follow the same trend. Both the curves were smoothed with fine averaging to remove the greater part of the oscillations due to possible TFBG signal fluctuations caused by high-heat transfer, transverse strains, OF bending, power detection accuracy and background noise. As the RI is obtained from the envelope area through the correlation fitting function, their trend is very similar. This means that both the envelope area and RI can provide information about the resin curing state as is demonstrated in Figure 7 for the RI variation trend. Hence, in an on-line monitoring application of the resin curing process, the envelope area trend provides enough information to determine the resin state without the RI calculation. However, since the RI has a physical meaning, it is preferred here to base the following discussion on its correlation with the resin cure degree.

In Figure 7, α and the resin RI curves are compared and three ranges were identified. In the first, the sensor measures the resin's RI monotone increasing due to the crosslinking of the polymeric chains. Though the initial RI variation is severe, the curve slope becomes milder quickly reflecting the slow resin crosslinking reaction occurring at room temperature. In the second range, the RI trend changes when the ramp-up is performed by switching-on the oven with the programmed temperature profile. The RI value detected from the TFBG at the start of the oven ignition is ∼1.552. This value deviates slightly from the one reported in the manufacturer data sheet for three main reasons: different reference temperature (here, ∼21 °C), the resin was previously mixed with its designated hardener which influences the overall RI, and the resin has already undergone part of the cure stage at room temperature. Switching-on the oven, the RI tends to flatten, and then decreases as the overall expansion due to the CTE of the mostly uncured resin dominates the shrinkage effect due to the crosslinking. Therefore, the RI curve reaches a local minimum point, where the third range starts. Here, the RI trend reverses when the degree of cure is about 0.4 which indicates that the resin system might be approaching its gelation point, and starts to increase as shrinkage related effect starts to dominate over the CTE. The competing effects between shrinkage and CTE in composite manufacturing has been discussed and quantified by means of FEA in [15]. The resin's RI converges into a plateau in the last part of the curing stage (observed also in [27,39]), where the great

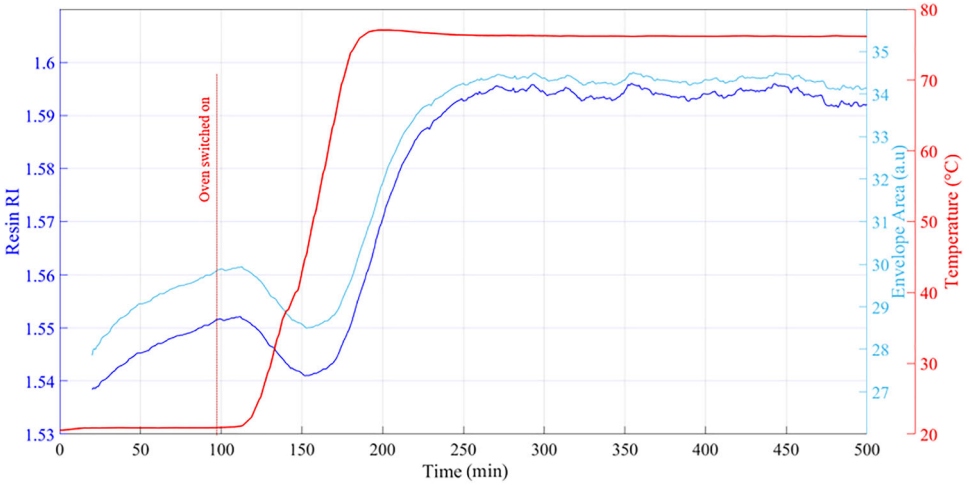

Figure 6. Resin RI measurement and envelope area trend during the composite curing time through the TFBG sensor with TC temperature.

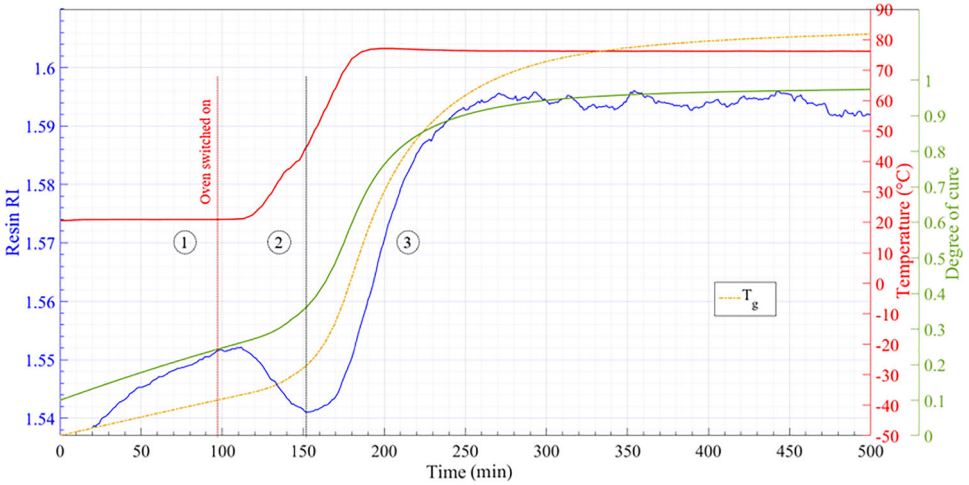

Figure 7. Comparison between α and the resin RI with TC temperature and T_g evolution.

part of the crosslinking reactions (α = 92%) occurred. The oscillations in the signal are possibly caused by the low crosslinking density occurring in this range, whereby the resin RI changes are too small to be detected from the TFBG with respect to the RI variation caused by the small temperature fluctuations. Hence, the resin RI measurements during its curing (or cladding resonance peaks envelope area), can be used to detect the different cure dynamics even without the help of the α curve. Additionally, a correlation between the resin RI and its degree of cure can be establish [40]. Furthermore, since the RI is sensitive to the temperature variations, its measurement can identify also whether the curing occurs at room temperature or in an oven. Finally, the resin's T_g is exceeding the curing temperature at about 330 min (Figure 7), leading to a vitrification of the matrix.

5. Conclusions

In this work, the TFBG sensor has been demonstrated to be able to act as a three-parameter OF sensor in monitoring the VARTM manufacturing process of a glass-fibre/epoxy composites. The TFBG proved to be useful in detecting the time needed by the resin flow front to reach the TFBG and the envelope area can be also used to obtain flow information as resin arrival time, infusion degree and poor resin wetting. The TFBG simultaneous strain-temperature measurements detected during the curing in the oven, indicated a relevant development of compressive strains during cool-down. The measured temperature matches well the one detected by the TC. However, the two profiles deviated due to the TFBG thermal resolution, which influences also the measured strains. This limitation can be easily overcome using a FBG interrogator with a higher *swR*. The maximum strain deviation calculated corresponds to 2.7% of the average strain for a short time interval of the curing step, and this value can be considered low. At the same time, The TFBG spectra provide the resin RI variation starting from the infusion step. The comparison of the RI trend with the resin degree of cure obtained from its cure kinetics, showed that the RI measurements

can detect the resin cure state throughout the process. The monitoring technique can in future be applied to carbon fibre composites made with Liquid Composite Moulding processes or in an autoclave, and in pre-pregs composites. Furthermore, the TFBGs may be suitable for the composite industry as they can improve the quality and health control of the products by providing information during the manufacturing process and in service. TFBG measurements can be also performed on thicker composites, and can be potentially obtained in real-time, and for all the three dimensions of the composite by embedding more TFBGs.

To conclude, a single minimal intrusive TFBG sensor was demonstrated as three-parameter OF sensor embedded in a composite, to monitor the thermomechanical and cure state of the composite during the several steps of its manufacturing process after performing a preliminary calibration of the sensor. This allow to improve the monitoring and sensing technology state of art and raise the concept of structural health monitoring of a product.

Acknowledgments

We would like to thank our colleague Andrei Anisimov for his contribution and suggestions during the TFBGs characterisation. Also, a great thanks to the DEMO lab technicians (in particular Peter den Dulk) at the TU Delft Aerospace Engineering building and to the technicians of the DASML Composite lab.

Disclosure statement

No potential conflict of interest was reported by the authors.

Funding

This research was supported by the Operationeel Programma Zuid-Nederland (Op-Zuid) Project as part of the Dutch Composite Maintenance Centre (DCMC), supported by the Europees Fonds voor Regionale Ontwikkeling (EFRO) and the North Brabant province of the Netherlands.

ORCID

Luigi Fazzi http://orcid.org/0000-0001-6177-8615
Giacomo Struzziero http://orcid.org/0000-0002-8262-4508
Clemens Dransfeld http://orcid.org/0000-0003-2912-7534
Roger Michael Groves http://orcid.org/0000-0001-9169-9256

References

[1] Rajak DK, Pagar DD, Menezes PL, et al. Fiber-reinforced polymer composites: Manufacturing, properties, and applications. Polymers, 2019; 11(1667):1–2.
[2] Zhang YX, Yang CH. Recent developments in finite element analysis for laminated composite plates. Compos Struct. 2009;88(1):147–157.
[3] Bogetti TA, Gillespie JW. Process-induced stress and deformation in thick section thermoset composite laminates. J Compos Mater. 1992;26(5): 626–660.
[4] Patel N, Lee LJ. Modeling of void formation and removal in liquid composite molding. Part I: wettability analysis. Polym Compos. 1996;17(1):96–103.
[5] Hofer B. Fibre optic damage detection in composite structures. Composites, 1987;18(4).
[6] Rao YJ. Recent progress in applications of in-fibre Bragg grating sensors. Opt Lasers Eng. 1999;31(4): 297–324.
[7] Ferdinand P, Magne S, Dewynter-Marty V, et al. Applications of fibre Bragg grating sensors in the composite industry. MRS Bull. 2002;27(5):400–407.
[8] Chehura E, Skordos AA, Ye CC, et al. Strain development in curing epoxy resin and glass fibre/epoxy composites monitored by fibre Bragg grating sensors in birefringent optical fibre. Smart Mater Struct. 2005;14(2):354–362.
[9] Antonucci V, Giordano M, Cusano A, et al. Real time monitoring of cure and gelification of a thermoset matrix. Compos Sci Technol. 2006; 66(16):3273–3280.
[10] Blößl Y, Hegedüs G, Szebényi G, et al. Applicability of fiber Bragg grating sensors for cure monitoring in resin transfer molding processes. J Reinf Plast Compos. 2020;40(19-20): 701–713.
[11] Balvers JM. In situ strain & cure monitoring in liquid composite moulding by fibre Bragg grating sensors [PhD thesis]. Delft: TU Delft;2014.
[12] Thompson AJ, McFarlane JR, Belnoue JP-H, et al. Numerical modelling of compaction induced defects in thick 2D textile composites. Mater Des. 2020;196:109088.
[13] Struzziero G, Skordos AA. Multi-objective optimization of resin infusion. Adv Manuf Polym Compos Sci. 2019;5(1):17–28.
[14] Rai N, Pitchumani R. Optimal cure cycles for the fabrication of thermosetting-matrix composites. Polym Compos. 1997;18(4):566–581.
[15] Struzziero G, Teuwen JJE. A fully coupled thermo-mechanical analysis for the minimisation of spring-in and process time in ultra-thick components for wind turbine blades. Composites Part A. 2020;139:106105.
[16] Li M, Zhu Q, Geubelle PH, et al. Optimal curing for thermoset matrix composites: thermochemical considerations. Polym Compos. 2001;22(1): 118–132.
[17] Cavaleiro PM, Araujo FM, Ferreira LA, et al. Simultaneous measurement of strain and temperature using Bragg gratings written in germanosilicate and Boron-Codoped germanosilicate fibers. IEEE Photon Technol Lett. 1999;11(12): 1635–1637.,

[18] Shu X, Liu Y, Zhao D, et al. Dependence of temperature and strain coefficients on fiber grating type and its application to simultaneous temperature and strain measurement. Opt Lett. 2002;27(9):701–703.,
[19] Montanini R, D'Acquisto L. Simultaneous measurement of temperature and strain in glass fibre/epoxy composites by embedded fibre optic sensors: I. Smart Mater Struct. 2007;16(5):1718–1726.
[20] de Oliveira R, Ramos CA, Marques AT. Health monitoring of composite structures by embedded FBG and interferometric Fabry-Perot sensors. Comput Struct. 2008;86(3-5):340–346.
[21] Kang HK, Kang DH, Bang HJ, et al. Cure monitoring of composite laminates using fibre optic sensors. Smart Mater Struct. 2002;11(2):279–287.
[22] Kang HK, Kang DH, Hong CS, et al. Simultaneous monitoring of strain and temperature during and after cure of unsymmetric composite laminate using fibre-optic sensors. Smart Mater Struct. 2003;12(1):29–35.
[23] Patrick HJ, Williams GM, Kersey AD, et al. Hybrid fibre Bragg grating/long period fibre grating sensor for strain/temperature discrimination. IEEE Photon Technol Lett. 1996;8(9):1223–1225.
[24] Triollet S, Robert L, Marin E, et al. Discriminated measures of strain and temperature in metallic specimen with embedded superimposed long and short fibre Bragg gratings. Meas Sci Technol. 2011;22(1):015202.,
[25] Albert J, Shao L, Caucheteur C. Tilted fibre Bragg grating sensors. Laser Photonics. 2013;7(1):83–108.
[26] Alberto NJ, Marques CA, Pinto JL, et al. Three-parameter optical fibre sensor based on a tilted fibre Bragg grating. Appl Opt. 2010;49(31):6085–6091.
[27] Buggy S, Chehura E, James S, et al. Optical fibre grating refractometers for resin cure monitoring. J Opt A: Pure Appl Opt. 2007;9(6):S60–S65.,
[28] Erdogan T. Fiber Bragg spectra. J Lightwave Technol. 1997;15(8)
[29] Erdogan T, Sipe J. Tilted fibre phase gratings. J Opt Soc Am A. 1996;13(2):296–313.
[30] Lee KS, Erdogan T. Fiber mode coupling in transmissive and reflective tilted fiber gratings. Appl Opt. 2000;39(9):1394–1404.
[31] Fazzi L, Groves RM. Demodulation of a tilted fibre Bragg grating transmission signal using α-shape modified delaunay triangulation. Measurement. 2020;166:108197.
[32] Antonucci V, Giordano M, Nicolais L, et al. Resin flow monitoring in resin film infusion process. J Mater Process Technol. 2003;143-144:687–692.
[33] Fazzi L, Valvano S, Alaimo A, et al. A simultaneous dual-parameter optical fibre single sensor embedded in a glass fibre/epoxy composite. Compos Struct. 2021;270:114087:1–12.
[34] Hexion Technical Information. https://www.swiss-composite.ch/pdf/t-Hexion-Harz-EPR04908.pdf (Last access 20/07/2021).
[35] Fazzi L, Groves RM. Refractometric properties of a TFBG sensor demodulated using α-Shape modified Delaunay triangulation. Optics. 2021;2(2):113–133.
[36] Su W-F, Fu Y-C, Pan W-P. Thermal properties of high refractive index epoxy resin system. Thermochim Acta. 2002;392–393:385–389.
[37] Khoun L, Centea T, Hubert P. Characterisation methodology of thermoset resins for the processing of composite materials — case study: CYCOM 890RTM epoxy resin. J Compos Mater. 2010;44(11):1397–1415.
[38] DiBenedetto AT. Prediction of the glass transition temperature of polymers: a model based on the principle of corresponding states. J Polym Sci B Polym Phys. 1987;25(9):1949–1969.
[39] Rajan G, Prusty BG, Health Monitoring Using S. Fiber optic methods. Boca Raton: CRC Press Taylor & Francis Group; 2017; p. 238–243.
[40] Dimopoulos A, Buggy SJ, Skordos AA, James SW, Tatam RP, Partridge IK. Monitoring cure in epoxies containing carbon nanotubes with an optical-fiber Fresnel refractometer. J Appl Polym Sci. 2009;113:730–735.